Research Journal of Applied Sciences, Engineering and Technology 7(2): 396-402, 2014
DOI:10.19026/rjaset.7.267
ISSN: 2040-7459; e-ISSN: 2040-7467

Submitted: April 22, 2013 Accepted: May 03, 2013 Published: January 10, 2014

Research Article

Framework to Harvest Waste Heat from Microprocessor using MEMS Thermoelectric Generator

[1]Tai Zhi Ling and [2]Ong Hang See
[1]Asia R and D Software and Firmware Development, Western Digital Malaysia, Jalan SS 8/6, Sungai Way, 47300, Petaling Jaya, Selangor
[2]Department of Electronics and Communication Engineering, Universiti Tenaga Nasional, Km7, Jalan Kajang Puchong, Kajang, Selangor

Abstract: The world primary energy consumption has been growing steadily. Therefore, there is a need to improve the overall energy application. There is a lack of investigation on harvesting waste heat from microprocessor as an alternative energy source. This study focuses on the framework required to harvest the energy from the microprocessor. Thermal profiling of the microprocessor integrated with an MEMS Thermoelectric Generator (TEG) using shunt configuration is developed. Additionally, a non-uniform energy model is derived to estimate the amount of energy that can be harvested from the microprocessor in the shunt configuration. MATLAB simulation based on the thermal and energy model is presented with two types of heat spreader material, copper and pyrolytic graphite with ideal and non-ideal contacts. The advantages and their shortfalls with respect to the microprocessor heat dissipation and the effectiveness to generate a temperature gradient at the MEMS TEG are discussed.

Keywords: Energy harvesting, microprocessor, MEMS thermoelectric, thermal modeling

INTRODUCTION

According to Institute of Energy Economics, Japan through APEC, the primary world energy consumption is expected to grow up to 16,487 million tons in 2030 (APEC, 2006). Malaysia in the Tenth Malaysia Plan has committed to reduce the country energy consumption by 10% by 2020 (APEC Secretariat, 2010). One of the energy sources that lack investigation is using microprocessor thermal heat as an energy source (Zhou *et al*., 2008). The thermal energy that is generated by the microprocessor after it is converted to electrical energy can be channeled to other applications, hence improving the overall energy efficiency used.

Microprocessors are present in various applications from general purpose computing to datacenter. IDC Server Power and Cooling Expenses Report (Michael, 2009) forecast the total servers worldwide to grow to approximately 45 million in 2010. The increase number of servers deploy will increase the power consumption and heat dissipation as highlighted by Brill (2007). IBM z 196 with a 5.20 GHz processor produces a maximum heat dissipation of 93.16 kBtu/hr (IBM Redbooks, 2011). Therefore recovering the waste heat from the microprocessor is worth investigating.

The fundamental principle to convert thermal energy into electricity rests on the Seebeck effect. Seebeck effect describes an electromotive force (emf) that is produced when the junction of two materials are heated (Goldsmid, 2009). The concept of using TEG to harvest waste heat from the microprocessor was first proposed and patented by Edward (1995). Suski proposed to harvest the waste heat from the microprocessor by connecting the TEG thermally in serial with the microprocessor and the heat sink. However Solbrekken *et al*. (2004) show that Suski's configuration was inefficient and an alternative configuration was suggested by placing the TEG in parallel with the microprocessor. The aforementioned alternative configuration requires an additional heat sink and suffers from convective heat losses during heat transfer process from the source.

In this study, a new configuration where the TEG is integrated inside the microprocessor using shunt configuration is proposed as shown in Fig. 1. This configuration used the Integrated Heat Spreader (IHS) as a heat sink for the microprocessor die and the TEG. Since the TEG is placed in an encapsulated environment, the heat transfer from the heat source to the TEG will have a minimum convective heat loss.

In order to understand the capability of the new configuration, an analytical model is developed to model the temperature profile and the thermoelectric energy conversion. Simulation study for the effect of the TEG placement with respect to the distance from the heat source is carried out. Simulation results and

Corresponding Author: Tai Zhi Ling, Asia R and D Software and Firmware Development, Western Digital Malaysia, Jalan SS 8/6, Sungai Way, 47300, Petaling Jaya, Selangor

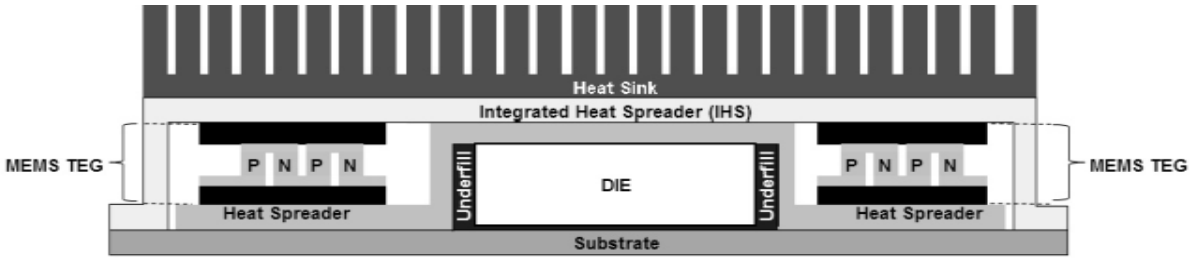

Fig. 1: MEMS TEG integrated in the processor

discussion shows an improvement for the energy density generated by the TEG with the new configuration.

MODELIN

Thermal modeling: Work presented by Yazawa *et al*. (2005), Xialong *et al*. (2010) and Fankai *et al*. (2011), proposed the thermal model where the geometric footprint of the TEG is similar with the heat sink. Since the heat sink footprint can be much bigger than the TEG, heat spreading effect should be considered. The spreading effect is considered in the works by Zhou *et al*. (2008) and Hsiao *et al*. (2010) Heat spreading equation is dependent on geometric structure as highlighted by Muzychka *et al*. (2003). Since the geometric structure of the shunt configuration is relatively complex, a new approach to model the heat transfer is needed.

Temperature difference occurs in a system will cause heat to be transferred from a higher temperature (heat source) to the lower temperature (heat sink) until equilibrium or steady-state is reached. Heat is transferred in a solid medium through conduction. The conduction is model at its steady state using Eq. (1) (Incropera and DeWitt, 2001):

$$Q'' = k\frac{\Delta T}{\Delta x} \tag{1}$$

In Eq. (1), Q" is the heat flux, k is the thermal conductivity of the material, ΔT is the temperature gradient and Δx is the total length between the temperature gradient. In order to convert to a 2 D conduction model, Eq. (1) is integrated to the first law of thermodynamics that is conservation of energy. The 2 D conduction equation at steady state can be described by Eq. (2):

$$k\frac{T_{x-1,y}-T_{x,y}}{\Delta x}\Delta y+k\frac{T_{x,y-1}-T_{x,y}}{\Delta y}\Delta x=k\frac{T_{x,y}-T_{x+1,y}}{\Delta x}\Delta y + k\frac{T_{x,y}-T_{x,y+1}}{\Delta y}\Delta x \tag{2}$$

In Eq. (2), k is the thermal conductivity, T_x and T_y are the temperatures at the location x, y and Δx and Δy are the total length between the temperature gradient at x-axis and y-axis respectively. In order to obtain rate of heat diffused into the material, the diffusivity rate is given by Eq. (3):

$$k\frac{T_{x-1,y,t}-T_{x,y,t}}{\Delta x}\Delta y+k\frac{T_{x,y-1,t}-T_{x,y,t}}{\Delta y}\Delta x = k\frac{T_{x,y,t}-T_{x+1,y,t}}{\Delta x}\Delta y+k\frac{T_{x,y,t}-T_{x,y+1,t}}{\Delta y}\Delta x + \rho c\Delta x\Delta y\left(\frac{T_{x,y,t+\Delta t}-T_{x,y,t}}{\Delta t}\right) \tag{3}$$

In Eq. (3), p is the density of the material, c is the heat capacity of the material and Δt is the time difference. In order to reach steady state, Eq. (3) is iterated until the temperature reaches equilibrium. Eq. (3) has a feedback mechanism therefore care must be taken to define the Δt to ensure that the system is stable at all times. Δt is constraint by Eq. (4):

$$\Delta t = \frac{1}{4}\times \alpha_{\min} \times \frac{1}{\Delta x\Delta y} \tag{4}$$

In Eq. (4), α_{min} is the minimum heat diffusivity of the material. Based on the Eq. (1) to (4), it is now possible to model the heat transfer of the microprocessor integrated with the MEM's TEG in shunt configuration.

The system is first partition into small discrete segments. The discrete segments which consist of Δx and Δy are defined based on the thinnest material used in the system. In order to simplify the simulation, Δx and Δy are made to be identical. Eq. (3) is not robust to handle complex geometric structures with segments which have incomplete unit squares and multiple materials with different thermal conductivity, density and heat capacity.

In order to overcome this, a single segment is partition into 4 smaller sub-segments with individual thermal conductivity at x and y axis as well as

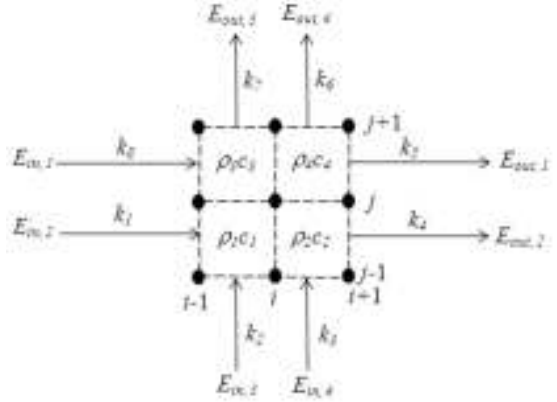

Fig. 2: Heat diagram of a single segment

individual density and heat capacity as shown in Fig. 2. The general equation can be represented in Eq. (5):

$$T_{i,j,t+\Delta t} = T_{i,j,t} + \frac{2\Delta t}{(\rho_1 c_1 + \rho_2 c_2 + \rho_3 c_3 + \rho_4 c_4)\Delta x^2}[(k_1 + k_8)T_{i-1,j,t} + (k_2 + k_3)T_{i,j-1,t} + (k_4 + k_5)T_{i+1,j,t} + (k_6 + k_7)T_{i,j+1,t} - \left(\sum_{n=1}^{8} k_n\right)T_{i,j,t}] \quad (5)$$

Energy generation modeling: Previous work from by Yazawa *et al*. (2005), Xialong *et al*. (2010) and Fankai *et al*. (2011), models the energy with a uniform temperature at the TEG surfaces. Temperature drop at the TEG substrate is also not considered for the energy model. Ananthanarayanan and Christopher (2010), show through simulation that the temperature at the heat spreader is non-uniform for a heat spreader connected in a shunt configuration with the heat source. The temperature non-uniformity will lead to inaccurate prediction of the TEG voltage generated using shunt configuration.

Zhou *et al*. (2008) developed an energy model taking into consideration of the non-uniform temperature distribution at the TEG surfaces. The energy model did not take into account substrate effects. Bongkyun *et al*. (2010), shows that the substrate affects the amount of energy generated by the TEG. For example, MPG-D751 MEM's TEG substrate thickness is 96% of the total thickness of the total thickness. This will lead to inaccuracy on the energy model if temperature drop is not considered. Therefore, a new energy model needs to be considered.

At steady state, the amount of heat entering the TEG will be equivalent to the heat dissipated from the TEG. At this state, a stable temperature gradient exists between the heat source and the heat sink. A general solution for an open circuit voltage is given by Eq. (6) is based on Zhou *et al*. (2008) with modification where in this case we assumed that there is different temperature on each element:

$$V_{OC} = \sum_{k=1}^{N}\left(\alpha_p \Delta T_{k,p} - \alpha_n \Delta T_{k,n}\right) \quad (6)$$

In Eq. (6), V_{OC} is the open circuit voltage, N is the total number of p-n thermoelectric elements, α_p and α_n is the Seebeck coefficient of the p and n thermoelectric element respectively and $\Delta T_{k,p}$ and $\Delta T_{k,n}$ is the k-th element average temperature gradient for the p and n element, respectively . The power received by the load from the TEG is given by Eq. (7):

$$P_L = \left(\frac{\sum_{k=1}^{N}\left(\alpha_p \Delta T_{k,p} - \alpha_n \Delta T_{k,n}\right)}{R_L + R_{pn}}\right)^2 R_L \quad (7)$$

In Eq. (7), R_L and R_{pn} are the load resistance and the p-n thermoelectric element resistance, respectively. In order to deliver the maximum load, the p-n thermoelectric element resistance and the load resistance need to be identical. The maximum power equation is defined by Eq. (8):

$$P_{L,\max} = \frac{\left(\sum_{k=1}^{N}\left(\alpha_p \Delta T_{k,p} - \alpha_n \Delta T_{k,n}\right)\right)^2}{4R_L} \quad (8)$$

SIMULATION

The simulation model is based Fig. 1 configuration. Non-ideal contact is simulated on the contact area (heat spreader and TEG surfaces) with teeth like structure as shown in Fig. 3. The configuration consists of three major elements. The first element is the microprocessor which is based on Intel Pentium 4, 3.40 GHz, LGA 775 microprocessor. The second element is the MEM's TEG, Micropelt MPG-D 751. The third element is the heat spreader-two types of hears spreaders are used in this study, copper and pyrolytic graphite.

The boundary condition is assumed to be uniform with a temperature of 65°C running at 84 W (Intel Corporation, 2004) at the microprocessor die. The heat sink surface is assumed to be uniform with an ambient temperature of 25°C (Mohammad *et al*., 2012). The remaining items in Fig. 3 such as the substrate and underfill are assumed to be an insulator with an adiabatic behavior in the model.

The mechanical properties that are critical in the simulation are described in the Table 1.
The distance of the TEG from the underfill edge is varied from 0.1 to 2.4 mm. The model is simulated through MATLAB. Since the geometric configuration is symmetrical, only one of the symmetry is analyzed. The subsequent subsection will discuss on the results and the optimum distance of TEG from the heat source for different type of heat spreader.

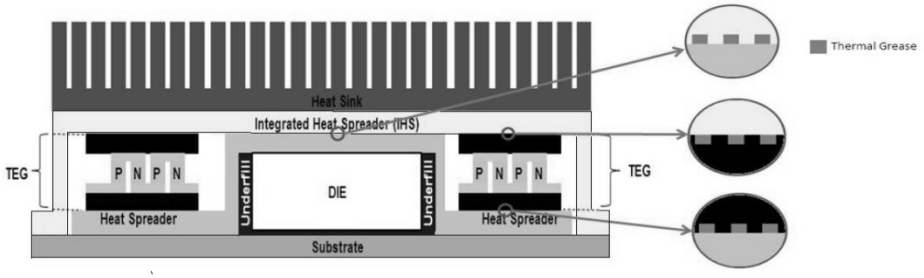

Fig. 3: Non-ideal structure on contact areas

Table 1: Mechanical properties used in simulation model

Component	Parameter	Value
Microproce	Die length[1]	13 mm
ssor	Die thickness[1]	1.1 mm
	Underfill gap (left and right)[1]	2 mm
	IHS nickel plating thickness[1]	0.1 mm
	IHS copper thickness[1]	0.8 mm
	Total Processor length[1]	29.2 mm
TEG	Substrate thickness[3]	0.525 mm
	TEG element thickness[3]	0.04 mm
	n-type element (Bi_2Te_3)[4]	-160 μV/K
	p-type element (Sb_2Te_3)[5]	195 μV/K
	TEG electrical resistance[3]	300 Ω
Heat	Spreader thickness	0.03 mm
spreader	Copper || thermal conductivity[2]	401 W/k-m
	Copper ⊥ thermal conductivity[2]	401 W/k-m
	PGS || thermal conductivity[6]	1600 W/k-m
	PGS ⊥ thermal conductivity[2]	5.70 W/k-m

[1]Estimated from a Pentium 4 LGA 775 Microprocessor; [2]Incropera and DeWitt (2001), [3]Micropelt (2007), [4]Bottner *et al*. (2004), [5]Wei-Chuan *et al*. (2009) and [6]Panasonic Industrial Co. (2011)

RESULTS AND ANALYSIS

Energy generation for MEM'S TEG attached in shunt configuration: In this subsection, the TEG shunt configuration using copper heat spreader is analyzed. First, the effect of the placement in relation to the energy conversion is investigated as shown in Fig. 3. As seen in Fig. 4 the energy conversion behavior towards the TEG distance can be divided to two parts. The first part indicated that a gradual energy conversion increase proportional to the distance. The second part meanwhile showed a gradual decrease proportional to the distance.

The first part is influenced by the TEG's cold surface (contacting the IHS). The TEG's cold surface temperature is contributed by the heat conducted through the TEG and the heat received from the IHS. The horizontal thermal resistance between the TEG's cold surface and the heat source will increase with the distance from the heat source. Therefore less heat will be received by the TEG's cold side from the IHS. This results in lower temperature on the TEG's cold surface. The lower temperature will increase the temperature gradient and energy generated.

The second part is influenced by the TEG's hot surface (contacting the heat spreader). The horizontal thermal resistance on the TEG's hot surface will also increase with the distance from the heat source.

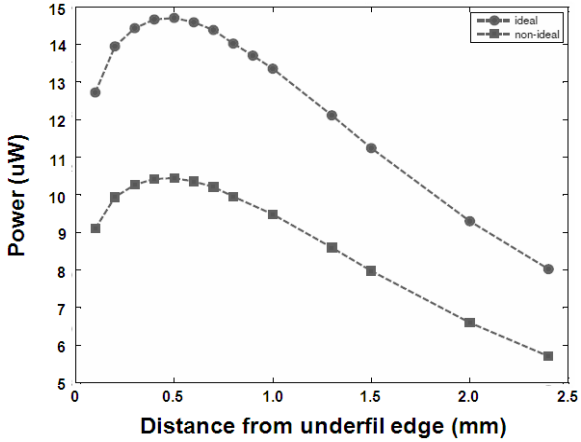

Fig. 4: Maximum power generated in TEG versus the distance from the underfill edge for copper spreader

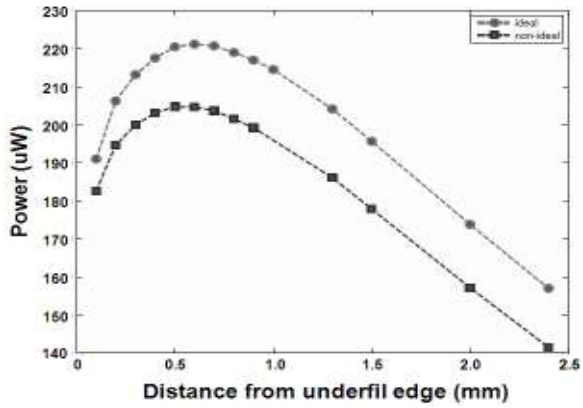

Fig. 5: Maximum power generated in TEG versus the distance from the underfill edge with pyrolytic graphite heat spreader

Therefore less heat will flow to the TEG's hot surface. As the distance of the TEG from the heat source continue to increase, the TEG's hot surface will have a lower temperature. As a result, the temperature gradient and energy generated will gradually decrease once the TEG's cold surface is unable to compensate for the temperature drop.

The highest amount of energy generated by a single TEG integrated with copper spreader is 14.7 uW at a distance of 0.5 mm from the source for ideal

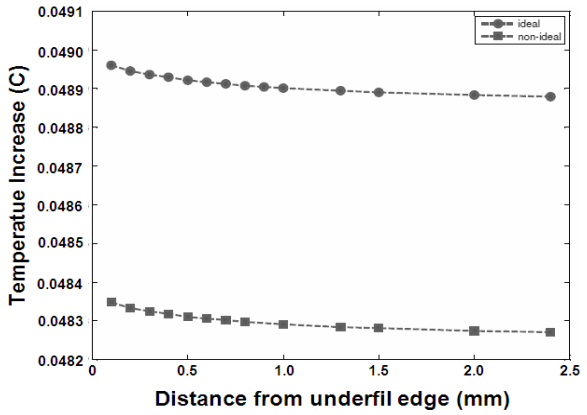

Fig. 6: Microprocessor die temperature increase versus the distance from the underfill edge using copper heat spreader

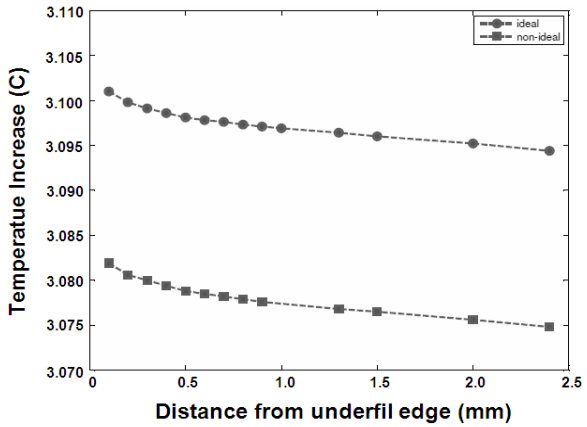

Fig. 7: Microprocessor die temperature increase versus the distance from the underfill edge using copper heat spreader

contact. Non-ideal contact is able to generate 10.45 μW at a distance of 0.5 mm from the source. The small amount of energy generated is attributed to a small average temperature gradient on the TEG.

Investigation is also carried out with pyrolytic graphite as a heat spreader. The effect of the TEG placement in relation to the energy conversion is shown in Fig. 5. Since the thermal conductivity of the pyrolytic graphite is approximately 4 times higher than copper the maximum energy generated by the TEG is 220.4 μW at a distance of 0.6 mm for ideal contact. Non-ideal contact has a maximum energy generated by the TEG is 204.7 μW at a distance of 0.5mm.

The experimental result from existing shunt configuration from Zhou *et al*. (2008) has a harvested energy density of 0.25 μW/mm^2. The proposed configuration improves the energy density from 0.91 to 18.23 μW/mm^2 depending on the heat spreader used with a non-ideal contact.

Heat dissipation for MEM'S TEG attached in shunt configuration: The microprocessor heat dissipation performance with relation to the TEG placement is explored as shown in Fig. 6. The temperature is observed to gradually increase as the TEG placement approach the heat source. This is because heat will be conducted from the heat spreader to the TEG's cold surface. As the TEG move closer to the source, the additional heat from the heat spreader will also increase. The presence of additional heat on the TEG's cold surface will reduce the IHS horizontal heat flow hence increasing the temperature of the microprocessor. As seen in Fig. 6, the heat spreader that is introduced has a maximum temperature increase of 0.04896°C and a temperature increase is 0.04892°C at the highest power generated for ideal contact. Non ideal contact has a maximum temperature increase of 0.04835°C and a temperature increase of 0.04831°C. Pyrolytic graphite heat spreader temperature dissipation is shown in Fig. 7. The maximum temperature increase of 3.101°C and 3.098°C at the highest power generated is registered for ideal contact. Non-ideal contact has a temperature of 3.0819°C and 3.0788°C is observed for TEG placement corresponding to the maximum temperature and power, respectively.

Pyrolytic graphite has relatively poor heat dissipation in comparison to copper heat spreader. Therefore, consideration on the poor heat dissipation needs to be taken into account prior to the integration of the pyrolytic heat spreader into the system design.

Application for waste heat energy harvested from microprocessor using MEM's TEG: The maximum simulated recycled energy is approximately 409.4μW for a single MEM's TEG with a non-ideal contact. Pentium 4 LGA 775 (Intel Corporation, 2004) has a package void area of 1248 mm^2. Therefore, allowing 4 MEM's TEG to be placed in the microprocessor. This implies that approximately 1.63 mW of energy can be recycled from the microprocessor.

The recycle energy is relatively small. One of the possible ways to reuse the recycled energy is to drive certain modules of the Central Processing Unit (CPU) during idle period. One example is to channel the energy to the Real Time Clock (RTC) and the Static RAM in the computer motherboard which consumes 15μW of energy (Intel Corporation, 2012). This will remove the need of replacing the CMOS battery in the microprocessor system resulting in a greener environment.

CONCLUSION

In this study, a model is presented to estimate the thermal profile of a microprocessor integrated the TEG with shunt configuration. Using the model two types of heat spreader are analyzed which are copper and

pyrolytic graphite integrated to the TEG. Result shows that pyrolytic graphite heat spreader is more effective in transferring heat to the TEG compare to copper.

The amount of energy harvested for two types of heat spreader is also analyzed for ideal and non-ideal contact for the system. The amount of energy generated is affected by the distance from the heat source where the optimum distance is between 0.5 to 0.6 mm. Pyrolytic graphite heat spreader configuration has the maximum amount of energy harvested from the TEG. The energy characteristic is similar for different types of heat spreader and contact. It is also noted that the heat dissipation of the processor does not vary significantly with the TEG placement.

Since the recycled energy is small, it can be used to drive low power applications such as replacing the CMOS battery operation on the motherboard.

REFERENCES

Ananthanarayanan, V. and C. Christopher, 2010. Theoretical study of conjugate heat transfer effects on temperature profiles in parallel flow with embedded heat sources. Int. J. Heat Mass Transfer, 53(9-10): 1699-1711.

APEC, 2006. Agency for natural resources and energy ministry of economy, trade and industry. Japan Oil, Gas and Metals National Corporation Fiscal 2005 Annual Energy Report (Outline), Japan.

APEC Secretariat, 2010. APEC Energy Overview 2009, Japan. Retrieved form: http:// publications. apec. org/ publication -detail.php?pub_id=1009.

Bongkyun, J., H. Seungwoo and K. Jeong-Yup, 2010. Optimal design for micro thermoelectric generators using finite element analysis. Microelectron. Eng., 88(5): 775-778.

Bottner, H., J. Nurnus, A. Gavrikov, G. Kuhner, M. Jagle and C. Kunzel, 2004. New thermoelectric components using micro system technologies. J. Microelectromech. Syst., 13(3): 414-420.

Brill K.G., 2007. The Invisible Crisis in the Data Center: The Economic Meltdown of Moore's Law, Uptime Institute. Retrieved form: http:// www. uptimeinstitute.org. (Accessed on: July 13, 2011)

Edward, S.D., 1995. Method and Apparatus for Recovering Power from Semiconductor Circuit Using Thermoelectric Device. US Patent #5,419780.

Fankai, M., C. Lingen and S. Fengrui, 2011. A numerical model and comparative investigation of a thermoelectric generator with multi-irreversibilities. Energy, 36(5): 3513-3522.

Goldsmid, H.J., 2009. Introduction to Thermoelectricity. Springer, Ch. 1, pp: 15-23.

Hsiao, Y.Y., W.C. Chang and S.L. Chen, 2010. A mathematical model of thermoelectric module with applications on waste heat recovery from automobile engine. Energy, 35(3): 1447-1454.

IBM Redbooks, 2011. IBM Zenterprise 196 Technical Guide. Vervante, pp: 354-355, ISBN: 0738436054, 9780738436050.

Incropera, F.P. and D.P. DeWitt, 2001. Fundamental of Heat and Mass Transfer. 5th Edn., John Wiley, New York.

Intel Corporation, 2004. Intel® Pentium® 4 Processor Supporting Hyper-Threading Technology Datasheet.

Intel Corporation, 2012. Intel ® I/O Controller Hub (Intel ® ICH/ Platform Controller Hub (PCH) Family Real Time Clock (RTC) Datasheet. Retrieved form: www.intel.pk/.../ich-family-real time-clock-accuracy-considerations-note.

Michael, B., 2009. The Economics of Virtualization: Moving toward an Application based Cost Model. IDC. Retrieved form: http:// www. vm ware. com/files/ pdf/ Virtualization-application-based-cost-model-WPEN.pdf.

Micropelt, G.B.H., 2007. MPG-D651, MPG-D751, Thin film Thermogenerators and Sensing Devices Datasheet. Retrieved form: http:// thermalforce. de/ engl/ product/ thermo generator/ micropelt_ d751.pdf.

Mohammad, Z.I., M.A. Miskam, M.N. Murat and M.A. Ahmad, 2012. Experimental investigation on cooling methods for micro thermoelectric power generator. Proceeding of the 3rd International Conference on Production, Energy and Reliability. KLCC, Kuala Lumpur, pp: 12-14.

Muzychka, Y.S., J.R. Culham and M.M. Yovanovich, 2003. Thermal spreading resistance of eccentric heat sources on rectangular flux channels. J. Electron. Pack, 125(2):178-185.

Panasonic Industrial Co., 2011. Retrieved form: http:// www. panasonic. com/ industrial/ electro niccomponents /protection/ heat- sinking- material. aspx. (Accessed on: September 23, 2011)

Solbrekken, G.L., K. Yazawa and A. Bar-Cohen, 2004. Thermal management of portable electronic equipment using thermoelectric energy conversion. Proceeding of the 9th Intersociety Conference on Thermal and Thermo mechanical Phenomena in Electronic Systems, ITHERM '04, pp: 276-283.

Wei-Chuan, F., L. Kuen-Ming and L. Min-Sheng, 2009. Large-scale preparation of ternary bisbte films with enhanced thermoelectric properties using dc magnetron sputtering. Proceeding of the 4th International Microsystems, Packaging, Assembly and Circuits Technology Conference (IMPACT 2009), pp: 457-460.

Xialong, G., X. Heng and Y. Suwen, 2010. Modeling, Experimental Study and Optimization on low temperature waste heat thermoelectric generator system. Appl. Energy, 87(10): 3131-3136.

Yazawa, K., G.L. Solbrekken and A. Bar-Cohen, 2005. Thermoelectric-powered convective cooling of microprocessors. IEEE T. Adv. Packaging, 28(2): 231-239.

Zhou, Y., S. Paul and S. Bhunia, 2008. Harvesting Wasted Heat in a Microprocessor Using Thermoelectric Generators: Modeling, Analysis and Measurements. Proceeding of the Design, Automation and Test in Europe (DATE '08), pp: 98-103.